

ARL 67-0223
NOVEMBER 1967



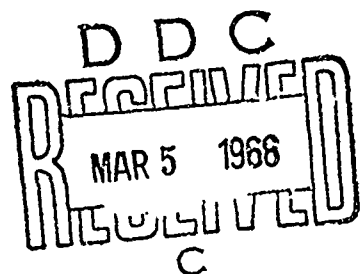
AD 665863

Aerospace Research Laboratories

COMPRESSIBLE TURBULENT PLANE COUETTE FLOW

ROBERT H. KORKEGI
RONALD A. BRIGGS, MAJOR, USAF
HYPERSONIC RESEARCH LABORATORY

Project No. 7064



This document has been approved for public release and sale;
its distribution is unlimited.

**OFFICE OF AEROSPACE RESEARCH
United States Air Force**



ARL 67-0223

COMPRESSIBLE TURBULENT PLANE COUETTE FLOW

**ROBERT H. KORKEGI
RONALD A. BRIGGS, MAJOR, USAF
HYPERSONIC RESEARCH LABORATORY**

NOVEMBER 1967

Project 7064

**This document has been approved for public
release and sale; its distribution is unlimited.**

**AEROSPACE RESEARCH LABORATORIES
OFFICE OF AEROSPACE RESEARCH
UNITED STATES AIR FORCE
WRIGHT-PATTERSON AIR FORCE BASE, OHIO**

FOREWORD

This report was prepared by Dr. Robert H. Korkegi and Maj Ronald A. Briggs of the Hypersonic Research Laboratory, Aerospace Research Laboratories, Office of Aerospace Research, United States Air Force. The investigation was carried out under Project 7064 entitled "High Velocity Fluid Mechanics."

ABSTRACT

Equations describing compressible turbulent plane Couette flow for the case of equal heat transfer at both walls have been developed for a perfect gas based on the von Karman mixing length model. This model was selected because of its good agreement with available turbulent plane Couette flow measurements of incompressible flow and furthermore, lacking compressible Couette flow data, it is shown by Spalding and Chi that those theories based on the von Karman model give best agreement with compressible turbulent boundary layer measurements.

A sample calculation is given for the heat rate to the inner surface of a rail-guided slipper (representative of slippers supporting rocket boosted sleds) based on the assumption of a small air gap between both surfaces.

TABLE OF CONTENTS

	PAGE
FOREWORD	ii
ABSTRACT	iii
LIST OF FIGURES	v
NOMENCLATURE	vi
INTRODUCTION	1
TURBULENT FLOW MODEL	1
GOVERNING EQUATIONS	2
INCOMPRESSIBLE CASE	5
DEDUCTIONS FROM THE INCOMPRESSIBLE LAW	6
COMPRESSIBLE CASE	8
REFERENCES	12

LIST OF FIGURES

FIGURE	PAGE
1. Sketch of Turbulent Plane Couette Flow	13
2. Theoretical Skin Friction and Heat Transfer Coefficients for Turbulent and Laminar Plane Couette Flow Compared with Experimental Data of Ref. 2	14
3. Incompressible Velocity Profiles Compared with Experi- mental Data of Ref. 2	15
4. Theoretical Skin Friction and Heat Transfer Coefficients for Turbulent Compressible Plane Couette Flow with Equal Wall Heating	16
5. Ratio of Compressible to Incompressible Skin Friction Coefficients for Various Re_b	17
6. Velocity Profiles for Turbulent Compressible Plane Couette Flow for Various Mach Numbers at $Re = 10^4$	18
7. Velocity Profiles for Turbulent Compressible Plane Couette Flow for Various Reynolds Numbers at $M_c = 4.0$	19
8. Density Profiles of Turbulent Plane Compressible Couette Flow for Various Mach Numbers at $Re_b = 10^4$	20
9. Enthalpy Profiles of Turbulent Plane Compressible Couette Flow for Various Mach Numbers at $Re_b = 10^4$	21
10. Sketch of Slipper in Proximity to Rail	22

NOMENCLATURE

b	half-gap height
C_f	local skin friction coefficient
C_h	local heat transfer coefficient
E	constant empirically determined
h	enthalpy
k_ϵ	eddy conductivity
l	mixing length
m	Eqn. 8
M	Mach number
M_c	Eqn. 8
p	pressure
Pr	Prandtl number
q	rate of heat transfer
R	gas constant
Re	Reynolds number
T	temperature
u	velocity
\bar{u}	u/u_c
u_τ	shear velocity
u^+	nondimensional velocity
y	distance from lower wall
y^+	nondimensional distance
κ	mixing length constant

μ eddy viscosity

τ shear stress

Subscripts

b half-gap

c properties at midpoint of gap

d gap width

r upper wall

t turbulent

w lower wall

ϵ eddy

∞ free stream

INTRODUCTION

Turbulent plane-Couette-like flow has been observed experimentally by Reichardt¹ and Robertson² in apparatus utilizing endless moving belts. Both authors, as well as Squire³, present theoretical treatments for the incompressible case.

Based on experimental evidence (cf. Refs. 2 and 4), turbulent plane Couette flow can be expected to occur at $Re_d \geq 0$ (10^3) where d denotes gap height. In the data of Couette, presented by Robertson², laminar flow was observed for $Re_d \leq 400$ and turbulent flow for $Re_d \geq 10^3$ between concentric cylinders with a spacing of 1.7% of the cylinder radius.

Interest in compressible turbulent plane Couette flow is stimulated by such problems as the rail-guided sliders supporting rocket-boosted sleds accelerated to speeds of several 1000 f. p. s. at the Test Track Directorate of AFMDC, Holloman AFB. Fully developed shear flows can be expected in the air gap between slider and rail surfaces, and the Reynolds numbers based on gap height are large enough for turbulent flow to prevail.

TURBULENT FLOW MODEL

For lack of experimental data on compressible turbulent plane Couette flow, the turbulent law selected is chosen as that which gives best agreement with turbulent boundary layer data at supersonic speeds, compatible with good agreement with the low speed skin friction and velocity profiles for turbulent Couette flow measured by Robertson². The data of Robertson were used because of the large number of measurements presented and their good agreement with the earlier work of Couette.

According to the excellent survey of theories for turbulent boundary layer flow of Spalding and Chi⁶, those based on mixing length give best agreement with experiment for both the adiabatic and nonadiabatic wall case. Two of the three theories giving best agreement are those of Wilson⁷ and Van Driest⁸, both based on the von Karman mixing length.

On the strength of these findings coupled with the good agreement with Robertson's data, the von Karman mixing length is selected as turbulent flow model.

GOVERNING EQUATIONS

For Couette flow the equations of motion reduce to

$$\text{Momentum} \quad \tau = \text{const} = \tau_w \quad (1)$$

$$\text{Energy} \quad q - \tau u = \text{const} = q_w \quad (2)$$

Where τ and q are taken to denote the sum of laminar and turbulent shear and heat transfer respectively, the subscript w denotes values at the lower wall, and u denotes the time average value of the velocity. A sketch of the flow is shown in Fig. 1.

Note that $\tau = \text{const}$ is a simplifying approximation in most turbulent boundary layer theories, whereas it is exact for Couette flow.

In the compressible analysis, only the symmetrical case of equal wall temperatures and heat rates will be considered, which implies the velocity profile will be antisymmetric about the midpoint of flow. Thus, following Fig. 1 and utilizing Eqns. 1 and 2

$$q_r = -q_w = \tau_w u_c \quad (3)$$

where $u_c = \frac{1}{2} u_r$ is the midpoint velocity, the subscript r denoting values at the upper wall.

Neglecting the laminar contribution to shear and utilizing the von Karman mixing length

$$\tau_w = \rho \ell^2 \left(\frac{du}{dy} \right)^2 ; \quad \ell = -\kappa \frac{\frac{du}{dy}}{\frac{d^2 u}{dy^2}}$$

where κ is a mixing length constant whose value is taken as 0.4^9 , one obtains the differential equation

$$\frac{d^2 u^+}{dy^+} + \kappa \left(\frac{\rho}{\rho_w} \right)^{1/2} \left(\frac{du^+}{dy^+} \right)^2 = 0 \quad (4)$$

where y^+ and u^+ are nondimensional height and velocity defined as follows

$$y^+ = \frac{u_T y}{\nu_w} = -\sqrt{\frac{C_f}{2}} \text{Re}_b \frac{y}{b} \quad (4a)$$

$$u^+ = \frac{u}{u_T} = -\sqrt{\frac{2}{C_f}} \frac{u}{u_c}$$

$u_T = \sqrt{\tau_w / \rho_w}$ is the shear velocity, and Reynolds number and skin friction coefficients are based on midpoint values, b and u_c -- see Fig. 1 -- and wall viscosity, and defined as follows

$$\text{Re}_b = \frac{u_c b}{\nu_w} ; \quad \frac{C_f}{2} = \frac{\tau_w}{\rho_w u_c^2} = \left(\frac{u_T}{u_c} \right)^2$$

With the boundary condition $u^+ (y^+ = 0) = 0$, the general solution of Eqn. 4 yielding the velocity profile between the fixed wall and the midpoint of the flow is

$$y^+ = C \int_0^{u^+} \exp \left\{ \kappa \int_0^{\xi} \left(\frac{\rho}{\rho_w} \right)^{1/2} d\xi \right\} du^+ \quad (5)$$

If one applies a second boundary condition of $(du/dy)_{y=0} = \tau_w / \mu_w$ at the wall, e. g.,

$$\frac{du^+}{dy^+} \Big|_{y=0} = 1$$

one obtains a constant of integration

$$C = 1. \quad (5a)$$

However, as the flow near the wall is dominated by laminar motion, one cannot rigorously apply a boundary condition based upon a turbulent shear flow model. Therefore, in accordance with standard turbulent boundary layer notation (cf. Spalding and Chi),

$$C = \frac{\kappa}{E}$$

is used where the value E is determined empirically. E/κ may be viewed as a scale or stretching factor on the coordinate y . Thus,

$$\frac{E}{\kappa} y^+ = \int_0^{u^+} \exp \left\{ \kappa \int_0^{\xi} \frac{\xi}{u^+} \left(\frac{\rho}{\rho_w} \right)^{1/2} d\xi \right\} du^+ \quad (6)$$

The density ratio ρ/ρ_w for the compressible case is related to the velocity distribution by means of the energy equation, Eqn. 2. Introducing an eddy viscosity μ_ϵ , eddy conductivity k_ϵ , and turbulent Prandtl number $Pr_\epsilon = cp \mu_\epsilon / k_\epsilon$, the turbulent shear and heat rate are written respectively

$$\tau_t = \mu_\epsilon \frac{du}{dy} \quad \text{and} \quad q_t = - \frac{k_\epsilon}{cp} \frac{dh}{dy} = - \frac{\mu_\epsilon}{Pr_\epsilon} \frac{dh}{dy}$$

Neglecting the laminar contribution, from Eqn. 1, $\tau_w = \mu_\epsilon (du/dy) = \text{const}$ hence $q = q_t = - (\tau_w / Pr_\epsilon) (dh/du)$, and therefore Eqn. 2 is written

$$\frac{\tau_w}{Pr_\epsilon} \frac{dh}{du} + \tau_w u = -q_w$$

Assuming $Pr_\epsilon = 1$, and introducing Eqn. 3 for the case of equal heat transfer, its solution is

$$h = h_w + u_c u - \frac{u^2}{2} \quad (7)$$

A Mach number, M_c , based on midpoint velocity and wall enthalpy is defined

$$m^2 = \frac{\gamma-1}{2} \quad M_c^2 = \frac{u_c^2}{2h_w} \quad (8)$$

Equation 7 can thus be written

$$\frac{h}{h_w} = 1 + m^2 (2\bar{u} - \bar{u}^2) \quad (7a)$$

where

$$\bar{u} = \frac{u}{u_c}$$

Now, limiting the analysis to the case of a perfect gas -- $p = \rho R T$ --, and noting that the pressure is constant throughout the Couette flow

$$\frac{\rho}{\rho_w} = \frac{T_w}{T} = \frac{h_w}{h} = \left[1 + m^2 (2\bar{u} - \bar{u}^2) \right]^{-1} \quad (9)$$

INCOMPRESSIBLE CASE

For $\rho = \rho_w = \text{const}$, the solution of Eqn. 6 is

$$\frac{u}{u_c} = \frac{1}{\kappa} \sqrt{\frac{C_f}{2}} \ln \left(1 + E \sqrt{\frac{C_f}{2}} \text{Re}_b \frac{y}{b} \right) \quad (10)$$

and the skin friction law ($u = u_c$ for $y = b$)

$$\sqrt{\frac{2}{C_f}} = \frac{1}{\kappa} \ln \left(1 + E \sqrt{\frac{C_f}{2}} \text{Re}_b \right) \quad (11)$$

Best fit with the experimental data of Robertson is obtained for $E = 8.8$ (Note that E varies from about 11 to 13+ in various turbulent boundary layer theories based on mixing length, cf. Ref. 6), and furthermore, since turbulent Couette flow has been observed only for $\text{Re}_b \gtrsim 10^3$ for which $(E \sqrt{C_f/2} \text{Re}_b) \gtrsim 200$, Eqn. 11 can be approximated as

$$\sqrt{\frac{2}{C_f}} = 2.5 \ln \left(8.8 \sqrt{\frac{C_f}{2}} \text{Re}_b \right) \quad (12)$$

or $\sqrt{\frac{2}{C_f}} = 5.44 + 2.5 \ln \left(\sqrt{\frac{C_f}{2}} \text{Re}_b \right)$

This equation is plotted in Fig. 2 and gives very good agreement with Robertson's ² measured values as well as those of Couette given in the same reference over the whole range of Re_b . Also shown in Fig. 2 is the laminar law $C_f \text{Re}_b = 2$. Note that Eqn. 12 is almost identical to the skin

friction law given by Robertson based on Reichardt's solution for the velocity distribution assuming a parabolic variation of eddy viscosity

$$\sqrt{\frac{2}{C_f}} = 5.5 + 5.75 \log_{10} \left(Re_b \sqrt{\frac{C_f}{2}} \right)$$

Velocity profiles from Eqn. 10 with $\kappa = 0.4$ and $E = 8.8$, are given in Fig. 3 for $Re_b = 10^3, 10^4$, and 10^5 and compared with Robertson's measurements for $Re_b = 10^4$.

DEDUCTIONS FROM THE INCOMPRESSIBLE LAW

If the velocity profile very close to the wall is examined, the log term in Eqn. 10 can be expanded for

$$\text{yielding } \frac{u}{u_c} = \frac{1}{\kappa} \sqrt{\frac{C_f}{2}} \left\{ E \sqrt{\frac{C_f}{2}} Re_b \frac{y}{b} + O \left[\left(E \sqrt{\frac{C_f}{2}} Re_b \frac{y}{b} \right)^2 \right] \right\}$$

$$\text{or } \frac{u}{u_c} \approx \frac{E}{\kappa} \frac{C_f}{2} Re_b \frac{y}{b} \quad (13)$$

which has the desired linear laminar character and precisely the laminar form for $E/\kappa = 1$ except that the velocity profile has a much steeper slope as $[(C_f/2) Re_b]_{\text{turb}} \gg 1$ compared with $[(C_f/2) Re_b]_{\text{lam}} = 1$.

It is thus found that the von Karman mixing length model, which depends only on the local flow characteristics, gives the features of a laminar sublayer when applied near a wall.

Also, taking the slope of the velocity profile from Eqn. 10

$$\frac{d \left(\frac{u}{u_c} \right)}{d \left(\frac{y}{b} \right)} = \frac{\frac{E}{\kappa} \frac{C_f}{2} Re_b}{1 + E \sqrt{\frac{C_f}{2}} Re_b \frac{y}{b}} .$$

At the wall

$$\left. \frac{d \left(\frac{u}{u_c} \right)}{d \left(\frac{y}{b} \right)} \right|_{y=0} = \frac{E}{\kappa} \frac{C_f}{2} Re_b$$

as from Eqn. 13 and at the midpoint $y = b$

$$\left. \frac{d \left(\frac{u}{u_c} \right)}{d \left(\frac{y}{b} \right)} \right|_{y=b} = \frac{\frac{E}{\kappa} \frac{C_f}{2} Re_b}{1 + E \sqrt{\frac{C_f}{2}} Re_b} \approx \frac{1}{\kappa} \sqrt{\frac{C_f}{2}}$$

It is also interesting to note the form of the eddy viscosity for the incompressible case obtained from the slope expressed above and rewritten as follows

$$\tau_w = \rho_w \left(\nu_w + \kappa u_T \frac{E}{\kappa} y \right) \frac{du}{d \left(\frac{E}{\kappa} y \right)}$$

Here again appears the laminar form and the constant E/κ as a scale or stretching factor. Note that the form of the eddy kinematic viscosity from von Karman's mixing length model is linear for incompressible Couette flow

$$\nu_T = \kappa u_T y$$

As a matter of interest, the ratio of turbulent to laminar viscosity is

$$\frac{\text{turbulent viscosity}}{\text{laminar viscosity}} = \frac{E u_T y}{\nu_w} = E \sqrt{\frac{C_f}{2}} Re_b \frac{y}{b}$$

Thus, the approximation made in Eqn. 12 corresponds to neglecting the laminar contribution to the shear.

The form of the eddy viscosity is actually not too important -- what is important is the scale. Thus, if a parabolic eddy viscosity distribution is taken, rather than a linear variation, i. e. $\nu_T = \kappa u_T y (1 - u/2b)$

(following Reichardt), the skin friction becomes

$$\sqrt{\frac{2}{C_f}} = \frac{1}{\kappa} \left(1 + \frac{2}{E} \sqrt{\frac{2}{C_f}} \frac{1}{Re_b} \right)^{-1} \ln \left(1 + E \sqrt{\frac{C_f}{2}} Re_b \right)$$

which differs from Eqn. 11 only by a second order term.

COMPRESSIBLE CASE

In a manner analogous with turbulent boundary layer development, it is assumed that the incompressible scale factor holds for the compressible case, i.e. $E = 8.8$.

Introducing Eqn. 9 for the density ratio into Eqn. 6, one obtains

$$\frac{E}{\kappa} y^+ = \int_0^{u^+} \exp \left\{ \kappa \sqrt{\frac{2}{C_f}} \int \bar{u} = \sqrt{\frac{C_f}{2}} u^+ [1 + m^2(2\bar{u} - \bar{u}^2)]^{-\frac{1}{2}} du \right\} du \quad (14)$$

Integration yields the velocity distribution

$$\left(1 + \frac{1}{\kappa^2} \frac{C_f}{2} m^2 \right) \left(E \sqrt{\frac{C_f}{2}} Re_b \frac{y}{b} \right) = \left\{ \sqrt{1 + m^2(2\bar{u} - \bar{u}^2)} \right. \\ \left. - \frac{1}{\kappa} \sqrt{\frac{C_f}{2}} m^2 (1 - \bar{u}) \right\} \exp \left\{ \kappa \sqrt{\frac{2}{C_f}} \frac{1}{m} \left[\sin^{-1} \frac{m}{\sqrt{1+m^2}} - \sin^{-1} \frac{(1-\bar{u})m}{\sqrt{1+m^2}} \right] \right\} \\ - 1 + \frac{1}{\kappa} \sqrt{\frac{C_f}{2}} m^2 \quad (15)$$

and the skin friction law ($\bar{u} = 1$, $y/b = 1$)

$$\left(1 + \frac{1}{\kappa^2} \frac{C_f}{2} m^2 \right) \left(E \sqrt{\frac{C_f}{2}} Re_b \right) = \sqrt{1+m^2} \exp \left(\kappa \sqrt{\frac{2}{C_f}} \frac{1}{m} \tan^{-1} m \right) \\ - 1 + \frac{1}{\kappa} \sqrt{\frac{C_f}{2}} m^2 \quad (16)$$

for compressible flow.

Eqn. 16 can be approximated in similar fashion as Eqn. 11 and written

$$\sqrt{\frac{2}{C_f}} = \frac{1}{\kappa} \frac{m}{\tan^{-1} m} \ln \left(\frac{1 + \frac{1}{\kappa^2} \frac{C_f}{2} m^2}{\sqrt{1+m^2}} e^{-\sqrt{\frac{C_f}{2}} Re_b} \right) \quad (16a)$$

Note that, as $m \rightarrow 0$, $(\tan^{-1} m/m) \rightarrow 1$, and Eqns. 15 and 16 reduce to the incompressible form of Eqns. 11 and 12 respectively.

Fig. 4 shows the compressible turbulent plane Couette flow skin friction law given by Eqn. 16a as well as the laminar one obtained assuming a linear viscosity-temperature relationship, and $Pr = 3/4$, for equal wall temperature and heat rates

$$\left(\frac{C_f Re_b}{2} \right)_{\text{lam}} = 1 + \frac{\gamma-1}{3} Pr M_c^2$$

Note that, contrary to the turbulent case, the laminar skin friction increases with Mach number due to increasing wall cooling.

Also shown in Fig. 4 is the heat transfer coefficient C_h whose definition is

$$C_h = \frac{q_w}{\rho_w u_c (h_w - h_b)}$$

where h_b is the midpoint enthalpy. From Eqn. 7 -- $h_b = h_w + u_c^2/2$ -- and Eqn. 3, it follows that $C_h = C_f$. Alternately, the heat transfer rate to the walls may be calculated directly from Eqn. 3.

$$q_r = -q_w = \frac{1}{2} C_f \rho_w u_c^3 \quad (17)$$

The ratio of compressible to incompressible skin friction coefficients for various Reynolds numbers is shown in Fig. 5.

Typical turbulent velocity profiles, given by Eqn. 15, are shown in Figs. 6 and 7 for various Mach numbers and Reynolds numbers. The density and enthalpy profiles, obtained from Eqns. 9 and 15, are shown in Figs. 8 and 9.

The very small variation of density across most of the profiles, as shown in Fig. 8, suggests that the simplifying approximation of assuming constant density at the midpoint value, ρ_b , in the integration of Eqn. 6 might be useful.

Thus, with $(\rho_b/\rho_w) = (1 + m^2)^{-1}$ from Eqn. 9, Eqn. 6 yields essentially the incompressible velocity profile modified for compressibility

$$\frac{u}{u_c} = \frac{1}{\kappa} \sqrt{\frac{C_f}{2}} \sqrt{1+m^2} \ln \left(1 + \frac{E \sqrt{\frac{C_f}{2}} Re_b}{\sqrt{1+m^2}} \frac{y}{b} \right) \quad (18a)$$

and an approximate skin friction law

$$\sqrt{\frac{2}{C_f}} \approx \frac{\sqrt{1+m^2}}{\kappa} \ln \left(\frac{E \sqrt{\frac{C_f}{2}} Re_b}{\sqrt{1+m^2}} \right) \quad (18b)$$

The velocity profiles given by Eqn. 18a are somewhat fuller than those given by Eqn. 15, with increasing departure at higher Mach numbers. As for the skin friction law, C_f , given by Eqn. 18b, is lower than that of Eqn. 16a by about 5% at $M_c = 1$, 15% at $M_c = 2$, and increases to about 40% at $M_c = 8$ for $10^3 \leq Re_b \leq 10^6$.

Example:

Consider a slipper bearing riding along a rail at supersonic speed with a small air gap between the slipper and rail surfaces so that, in cross section, the flow may be considered two dimensional in the first approximation. Assume that at some distance behind the leading edge of the slipper, the flow in the gap becomes fully viscous and Couette flow develops. A sketch of the longitudinal cross section is shown in Fig. 10 indicating the approximate bow shock of the slipper.

For purposes of illustration it is assumed that the air entering the gap traverses a normal shock portion of the bow shock, and the pressure in the gap is constant and corresponds to that behind a normal shock.

Assume $u_\infty = 4500$ f. p. s. so that $u_c = u_\infty / 2 = 2250$ f. p. s., and the gap height is $1/8"$ so that $b = 1/16"$. Taking atmospheric temperature as 70°F , $T_\infty = 530^\circ\text{R}$; the speed of sound, $a = \sqrt{\gamma R T_\infty} = 1128$ f. p. s., so $M_\infty = 4.0$ and $M_c = 2$.

From the normal shock relation for $\gamma = 1.4$

$$\frac{p_{\text{gap}}}{p_\infty} = \frac{28 M_c^2 - 1}{6}$$

Here, assuming atmospheric wall temperature for slipper and rail -- $T_w = T_\infty = 530^\circ\text{R}$ -- the wall density is

$$\rho_w = \frac{p_{\text{gap}}}{R T_\infty} = \frac{p_\infty}{R T_\infty} \left(\frac{28 M_c^2 - 1}{6} \right) \approx 0.0430 \frac{\text{slug}}{\text{ft}^3}$$

The Reynolds number based on b is

$$Re_b = \frac{\rho_w u_c b}{\mu_w} \approx 1.38 \times 10^6$$

so that the Couette flow can be expected to be turbulent.

For $M_c = 2$ and $Re_b = 1.38 \times 10^6$, the turbulent skin friction coefficient, as given by Fig. 4, is

$$C_f = .0014$$

The wall heat transfer rate, from Eqn. 17, is then

$$q_w = \frac{1}{2} \rho_w u_c^3$$

$$\approx 450 \frac{\text{Btu}}{\text{ft}^2 \text{sec}}$$

This heat rate is comparable to those experienced at the stagnation point of some bodies during reentry. For example, the stagnation heat rates to a Mercury capsule are approximately $200 \text{ Btu}/\text{ft}^2 \text{ sec}$.

REFERENCES

1. Reichardt, H., "On the Velocity Distribution in a Rectilinear Turbulent Couette Flow," Z. Angew. Mach. Mech., Special Supplement, 1956, pp. 26-29 (In German).
2. Robertson, J. M., "On Turbulent Plane-Couette Flow," Proc. 6th Midwestern Conference on Fluid Mechanics, University of Texas, Austin, 1959, pp. 169-182.
3. Squire, W., "A Unified Theory of Turbulent Flow. II Plane Couette Flow," Appl. Sci. Res., Sect. A, Vol. 9, 1960, pp. 393-410.
4. Rouse, H., "A General Stability Index for Flow Near Plane Boundaries," J. Aeronaut. Sci., Vol. 12, No. 4, Oct 1945, pp. 429-431.
5. Spalding, D. B. and Chi, S. W., "The Drag of a Compressible Turbulent Boundary Layer on a Smooth Flat Plate with and without Heat Transfer," J. Fluid Mech., Vol. 18, Part 1, Jan. 1964, pp. 117-143.
6. Wilson, R. E., "Turbulent Boundary-Layer Characteristics at Supersonic Speeds - Theory and Experiment," J. Aeronaut. Sci., Vol. 17, No. 9, Sep 1950, pp. 585-594.
7. Van Driest, E. R., "50 Years of Boundary Layer Theory," (Ed. H. Görtler and W. Tollmien), Braunschweig: F. Vieweg u. Sohn, 1955, p. 257.
8. Schlichting, H., Boundary Layer Theory, 4th ed., McGraw-Hill, New York, 1960, p. 490.

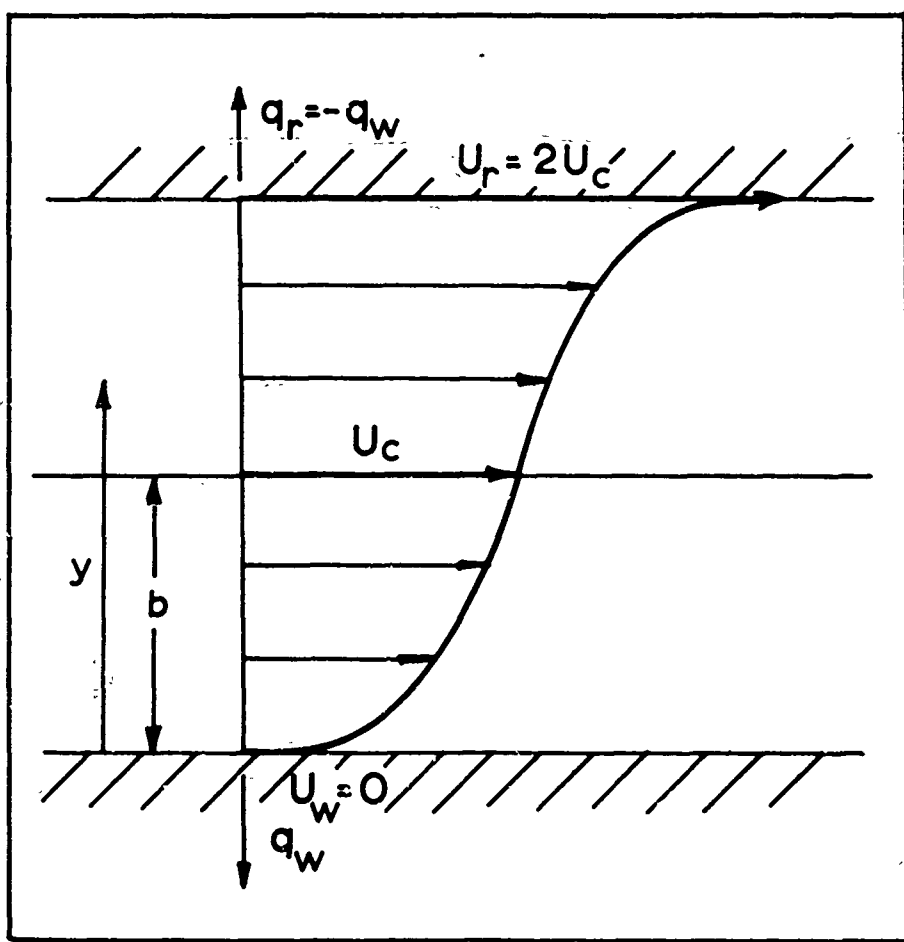


Fig. 1. Sketch of Turbulent Plane Couette Flow

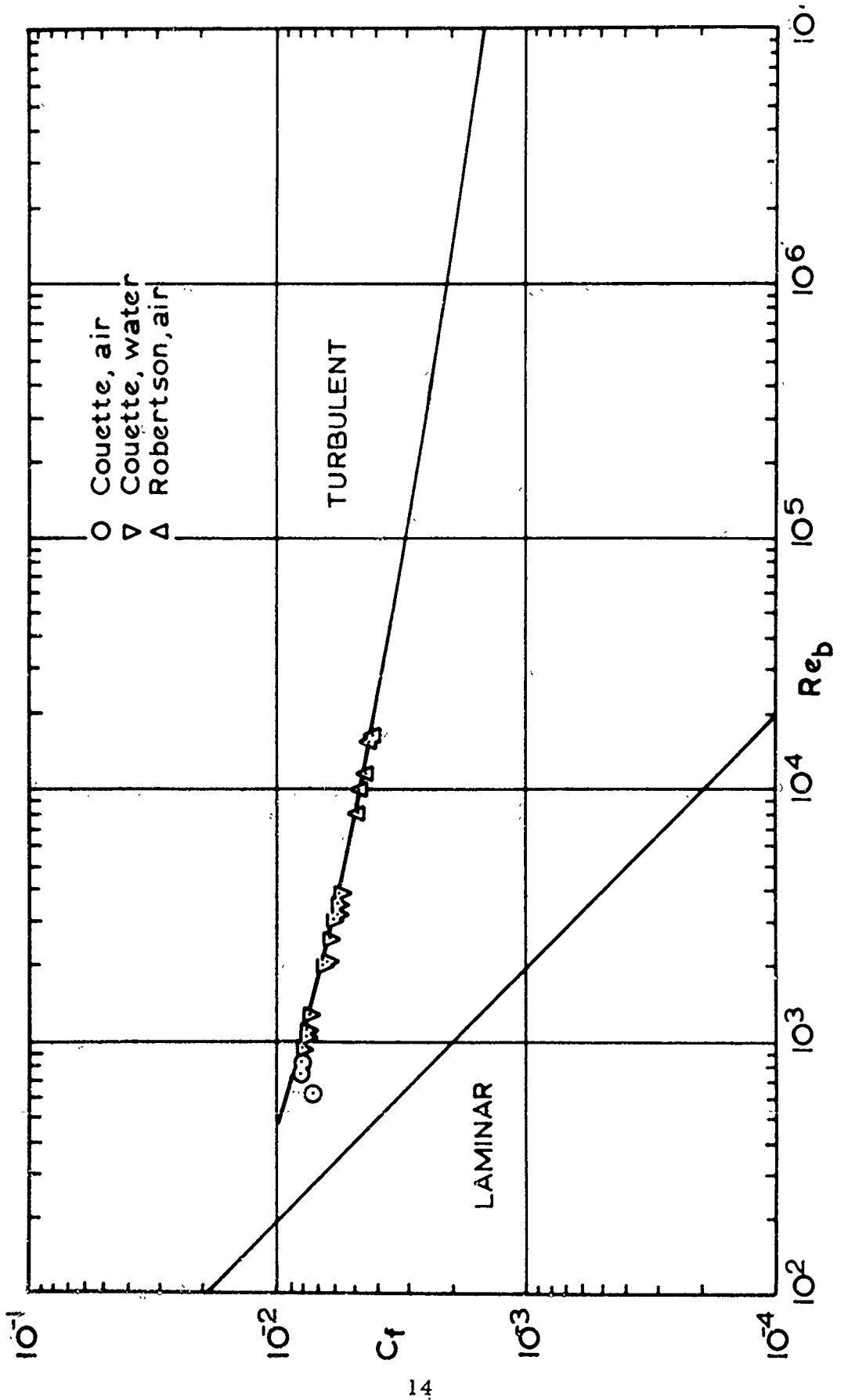


Fig. 2. Theoretical Skin Friction and Heat Transfer Coefficients for Turbulent and Laminar Plane Couette Flow Compared with Experimental Data of Ref. 2

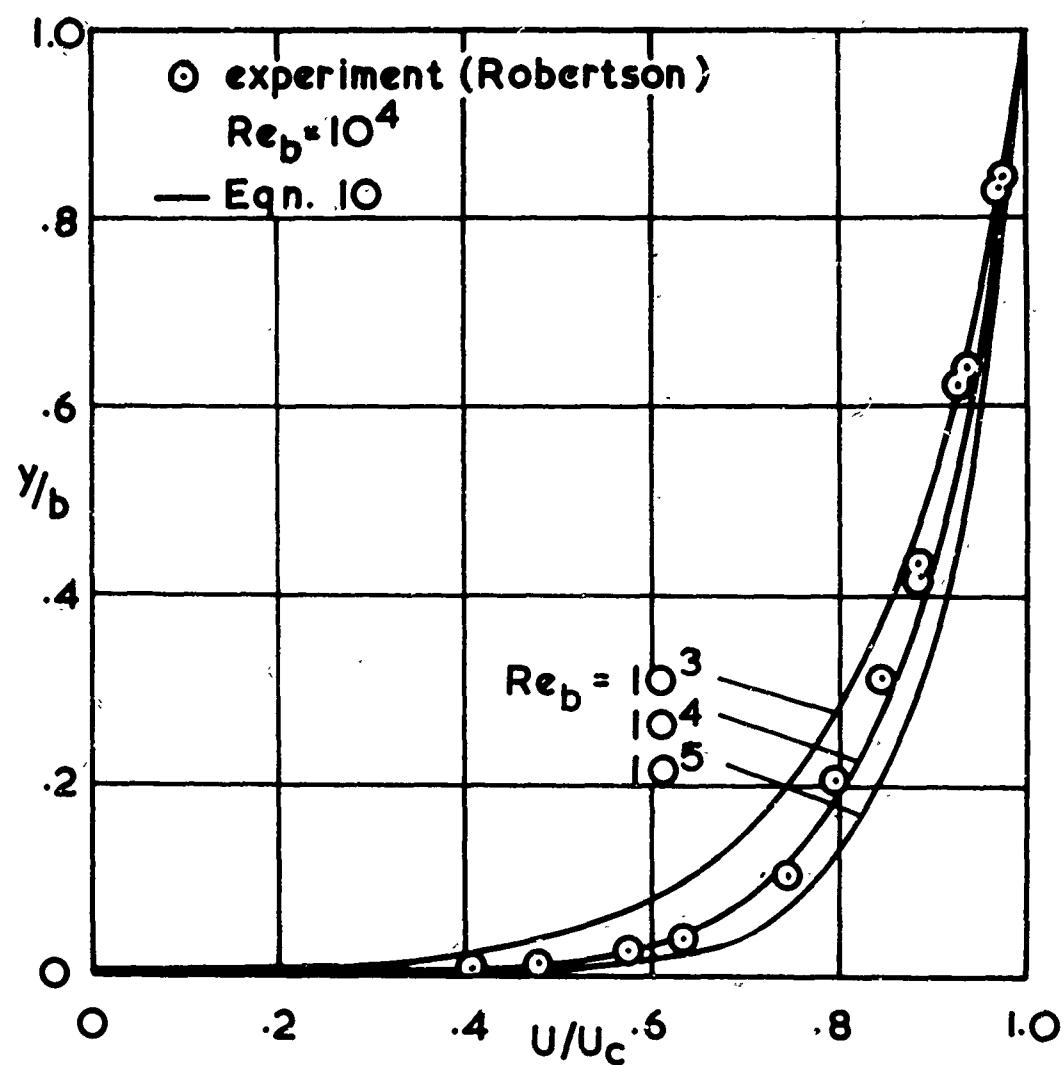


Fig. 3. Incompressible Velocity Profiles Compared with Experimental Data of Ref. 2

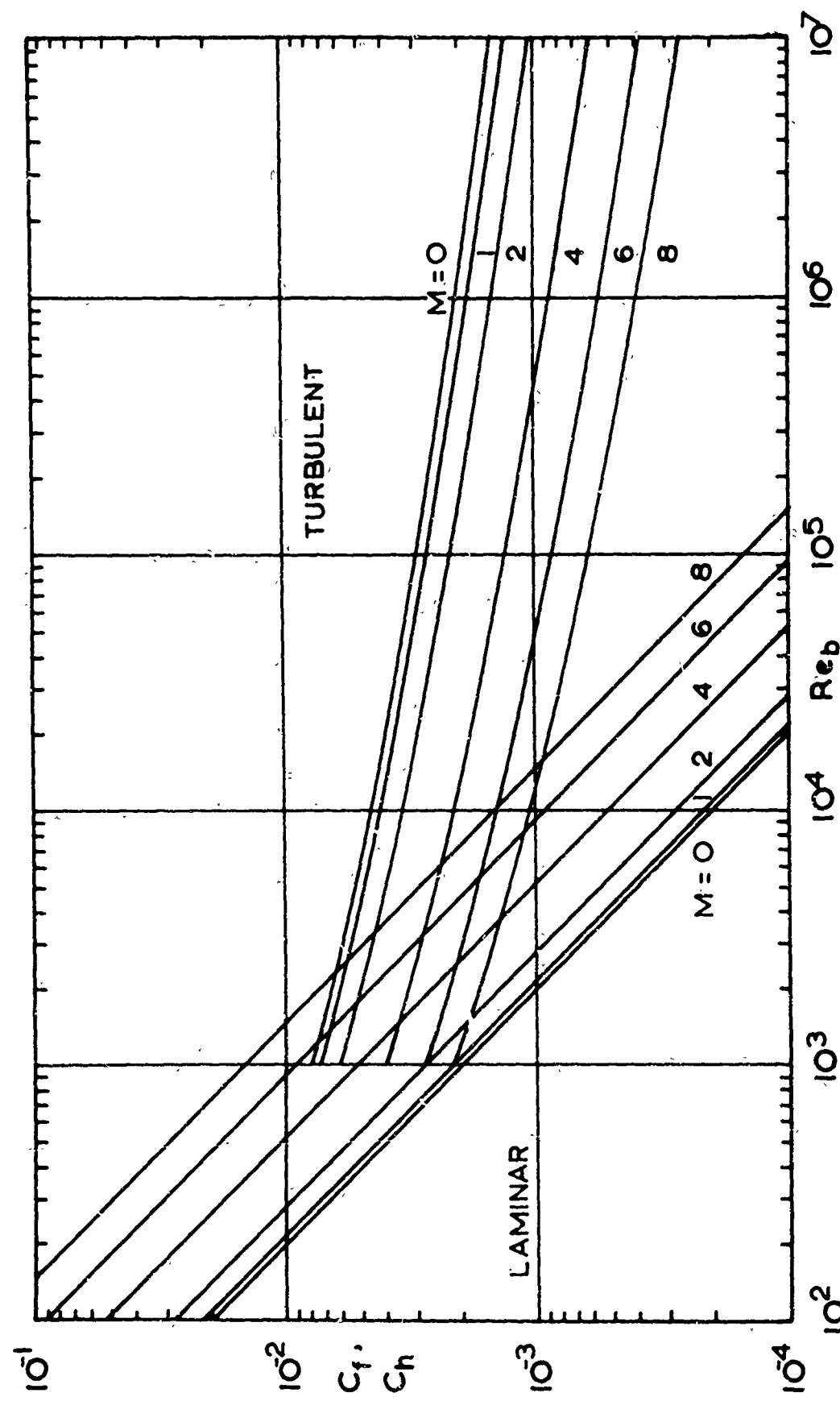


Fig. 4. Theoretical Skin Friction and Heat Transfer Coefficients for Turbulent Compressible Plane Couette Flow with Equal Wall Heating

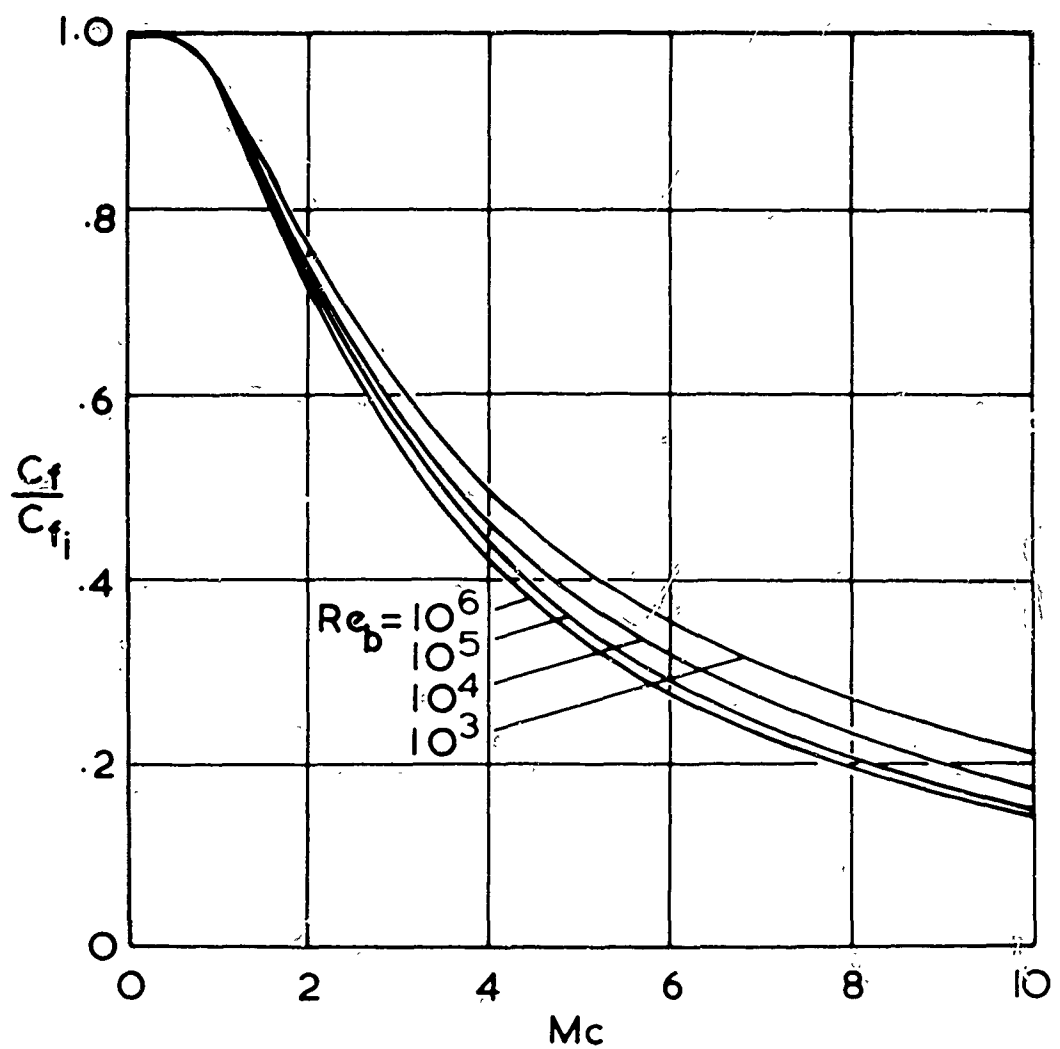


Fig. 5. Ratio of Compressible to Incompressible Skin Friction Coefficients for Various Re_b

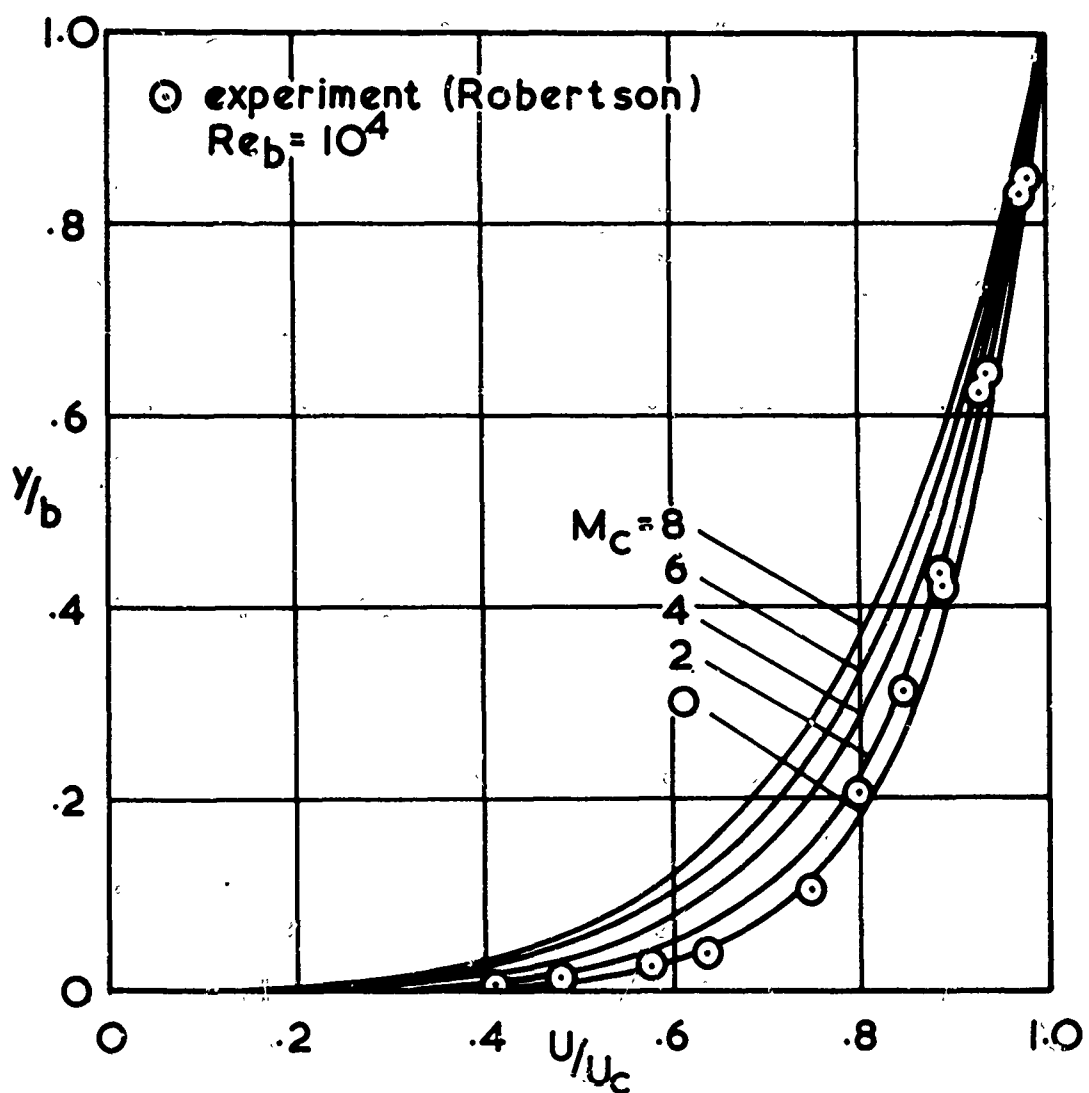


Fig. 6. Velocity Profiles for Turbulent Compressible Plane Couette Flow for Various Mach Numbers at $Re = 10^4$

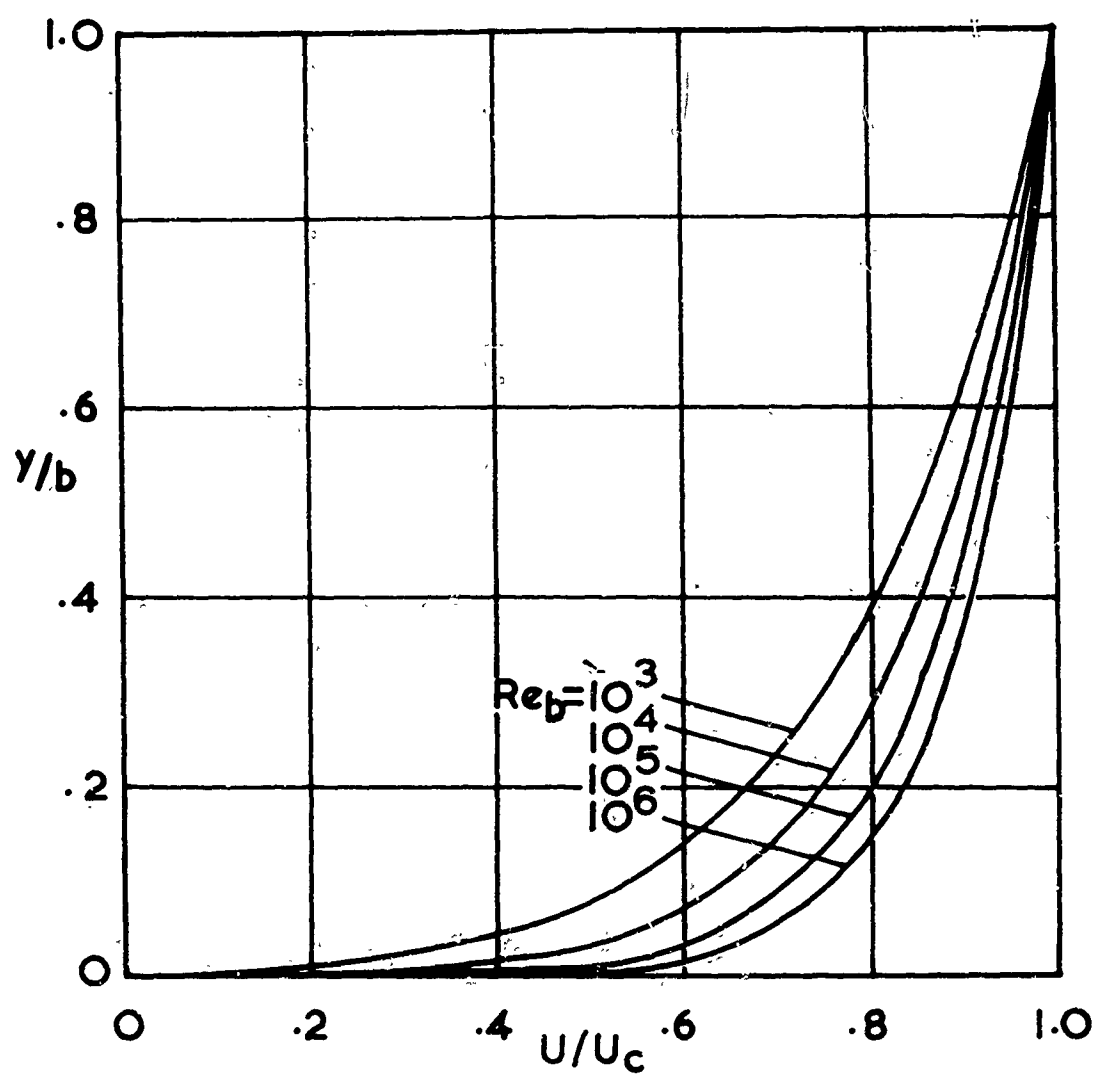


Fig. 7. Velocity Profiles for Turbulent Compressible Plane Couette Flow for Various Reynolds Numbers at $M_c = 4.0$

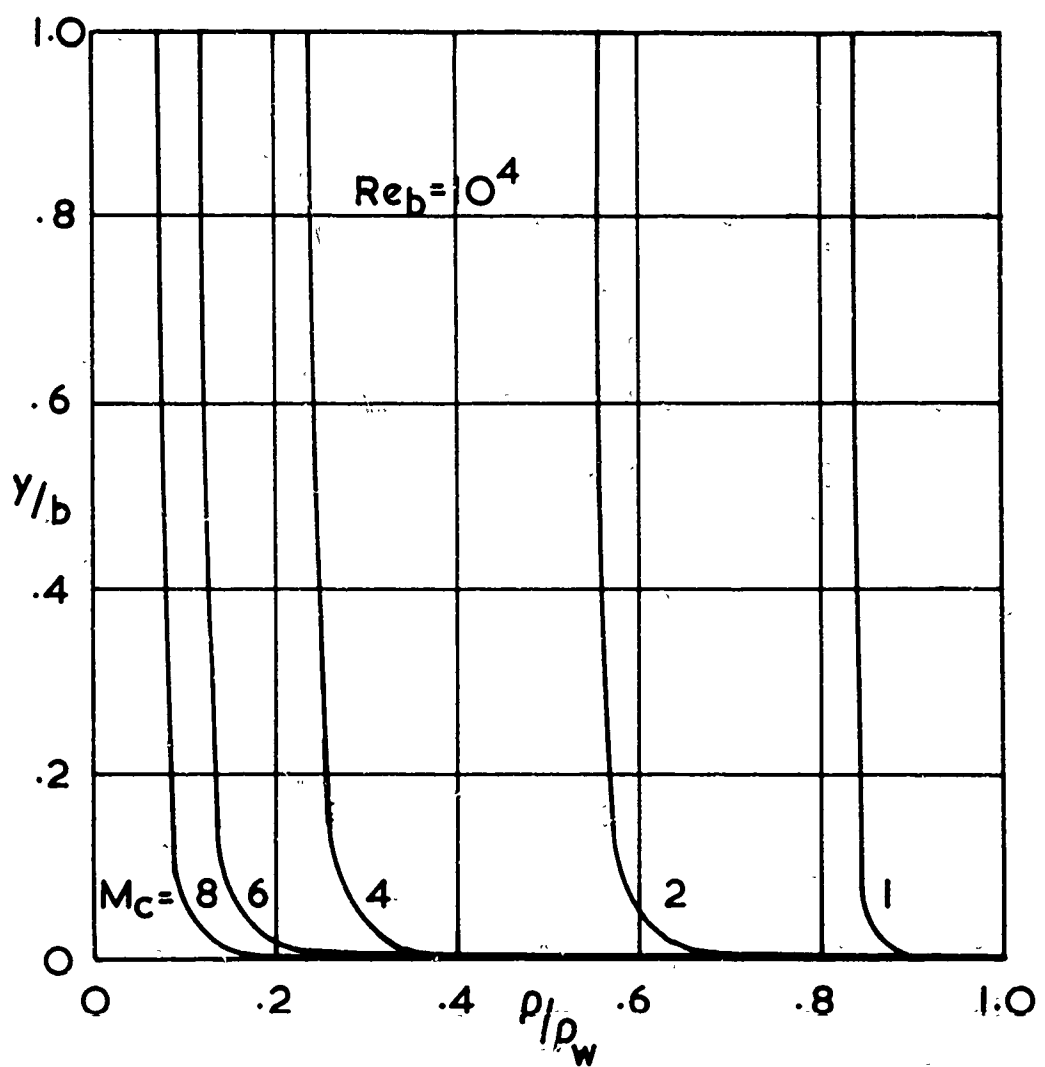


Fig. 8. Density Profiles of Turbulent Plane Compressible Couette Flow for Various Mach Numbers at $Re_b = 10^4$

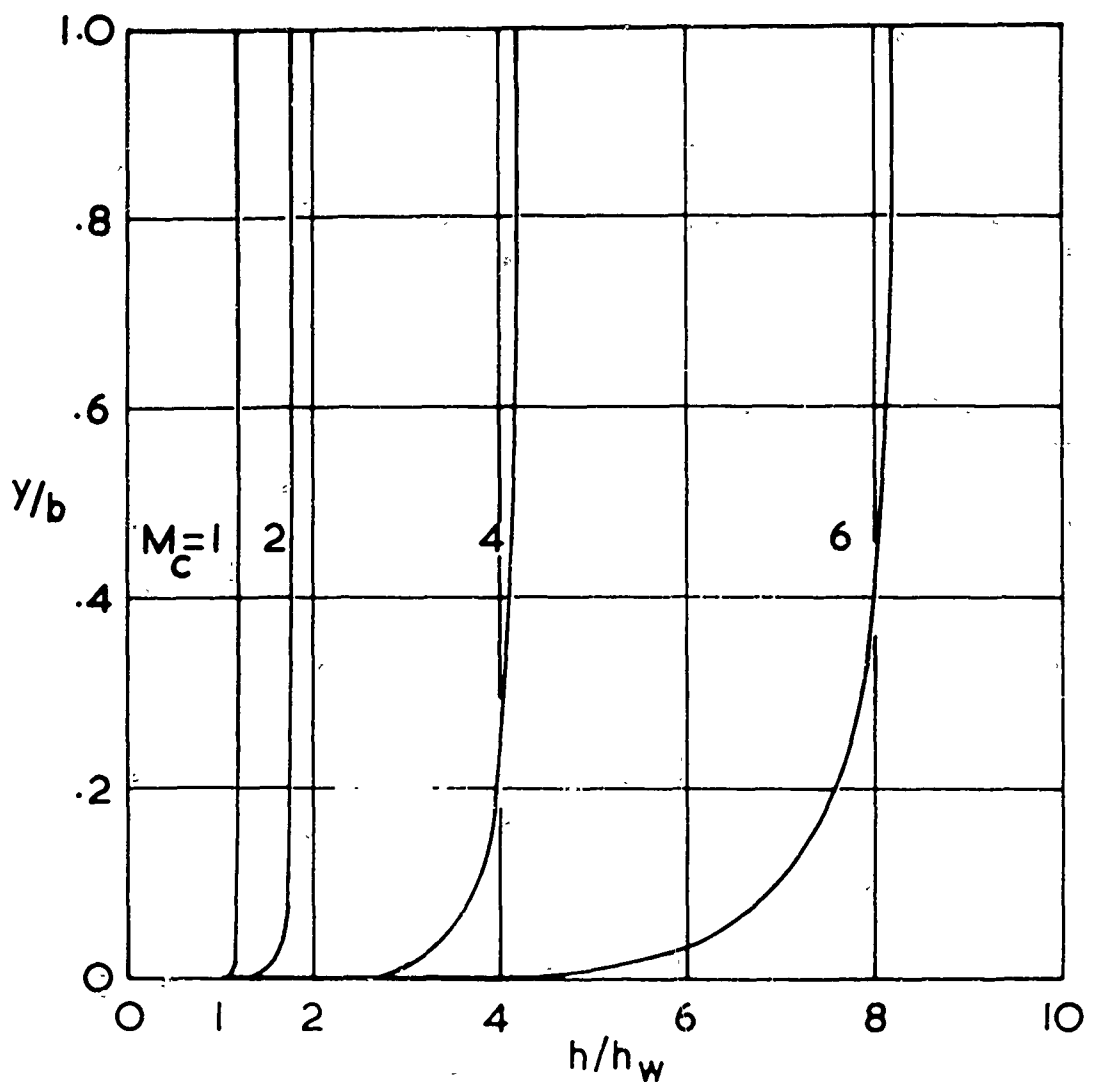


Fig. 9. Enthalpy Profiles of Turbulent Plane Compressible Couette Flow for Various Mach Numbers at $Re_b = 10^4$

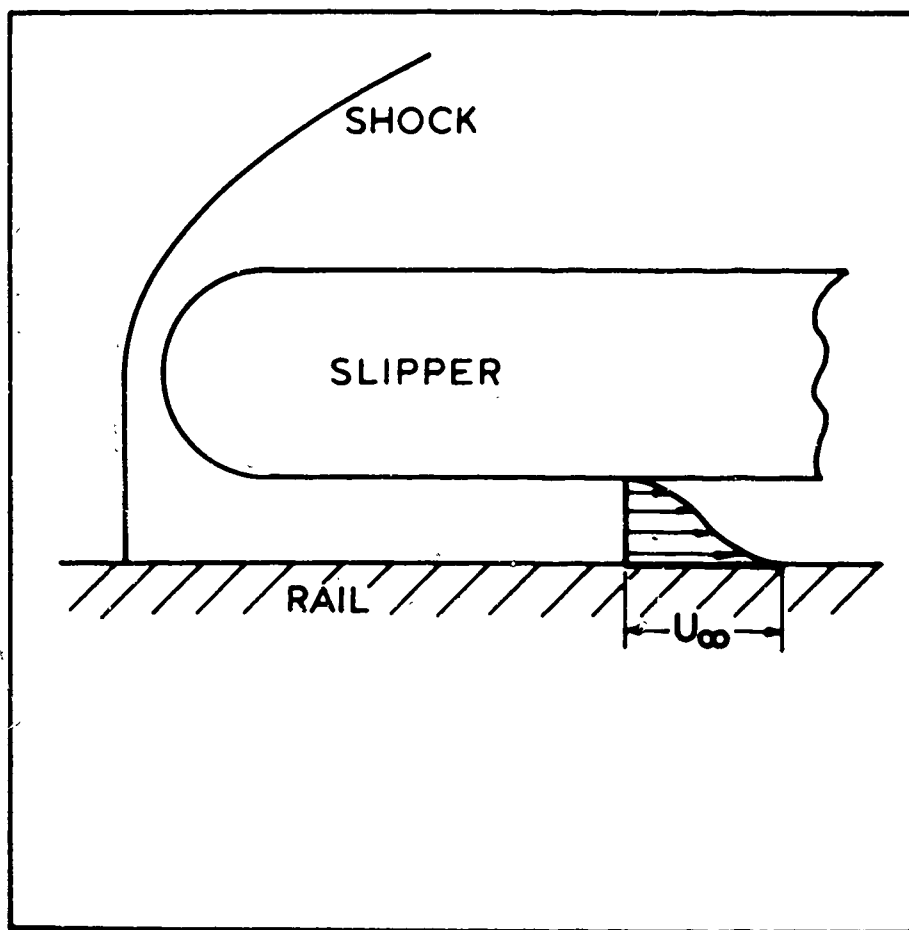


Fig. 10. Sketch of Slipper in Proximity to Rail

UNCLASSIFIED

Security Classification

DOCUMENT CONTROL DATA - R & D

(Security classification of title, body of abstract and indexing annotation must be entered when the overall report is classified)

1. ORIGINATING ACTIVITY (Corporate author) Aerospace Research Laboratories Hypersonic Research Laboratory Wright-Patterson AFB, Ohio 45433		2a. REPORT SECURITY CLASSIFICATION UNCLASSIFIED
2b. GROUP		
3. REPORT TITLE Compressible Turbulent Plane Couette Flow		
4. DESCRIPTIVE NOTES (Type of report and inclusive dates) Scientific Interim		
5. AUTHOR(S) (First name, middle initial, last name) Robert H. Korkegi Ronald A. Briggs		
6. REPORT DATE November 1967	7a. TOTAL NO. OF PAGES 22	7b. NO. OF REFS 8
8. CONTRACT NUMBER In-house Research		9a. ORIGINATOR'S REPORT NUMBER(S)
9. PROJECT NO. 7064-00-06		9b. OTHER REPORT NO(S) (Any other numbers that may be assigned (this report)) ARL 67-0223
c. DoD Element 61445014 d. DoD Subelement 681307		
10. DISTRIBUTION STATEMENT 1. This document has been approved for public release and sale; its distribution is unlimited.		
11. SUPPLEMENTARY NOTES TECH OTHER	12. SPONSORING MILITARY ACTIVITY Aerospace Research Laboratories (ARR) Wright-Patterson AFB Ohio 45433	
13. ABSTRACT Equations describing compressible turbulent plane Couette flow for the case of equal heat transfer at both walls have been developed for a perfect gas based on the von Karman mixing length model. This model was selected because of its good agreement with available turbulent plane Couette flow measurements of incompressible flow and furthermore, lacking compressible Couette flow data, it is shown by Spalding and Chi that those theories based on the von Karman model give best agreement with compressible turbulent boundary layer measurements.		
A sample calculation is given for the heat rate to the inner surface of a rail-guided slipper (representative of slippers supporting rocket boosted sleds) based on the assumption of a small air gap between both surfaces.		

DD FORM 1 NOV 65 1473

UNCLASSIFIED

Security Classification

UNCLASSIFIED

Security Classification

14. KEY WORDS	LINK A		LINK B		LINK C	
	ROLE	WT	ROLE	WT	ROLE	WT
Turbulent Boundary Layer						
Couette Flow						
Compressible Flow						
Heat Transfer						

UNCLASSIFIED

Security Classification